

Precise gene replacement in rice by RNA transcript-templated homologous recombination

Shaoya Li¹, Jingying Li¹, Yubing He², Meilian Xu², Jiahui Zhang¹, Wenming Du¹, Yunde Zhao^{1,3*} and Lanqin Xia^{1*}

One of the main obstacles to gene replacement in plants is efficient delivery of a donor repair template (DRT) into the nucleus for homology-directed DNA repair (HDR) of double-stranded DNA breaks. Production of RNA templates in vivo for transcript-templated HDR (TT-HDR) could overcome this problem, but primary transcripts are often processed and transported to the cytosol, rendering them unavailable for HDR. We show that coupling CRISPR-Cpf1 (CRISPR from *Prevotella* and *Francisella* 1) to a CRISPR RNA (crRNA) array flanked with ribozymes, along with a DRT flanked with either ribozymes or crRNA targets, produces primary transcripts that self-process to release the crRNAs and DRT inside the nucleus. We replaced the rice *acetolactate synthase* gene (*ALS*) with a mutated version using a DNA-free ribonucleoprotein complex that contains the recombinant Cpf1, crRNAs, and DRT transcripts. We also produced stable lines with two desired mutations in the *ALS* gene using TT-HDR.

Targeted, precise, genetic modification in plants has been difficult owing to a lack of efficient delivery of template DNA or RNA for HDR into the nucleus. Although protoplasts can be efficiently transformed, regeneration of plants from protoplasts is very inefficient¹. In general, double-stranded DNA breaks (DSBs) are repaired through either non-homologous end joining (NHEJ) or HDR. NHEJ is not precise and often causes random indels. In contrast, HDR is precise and can be used for gene replacement or other modifications. Carrying out HDR of DSBs in crops has proven challenging for two main reasons. First, NHEJ is the predominant pathway, while HDR is relatively rare². Second, delivery of DRT into plant cells is difficult to achieve. Both particle bombardment and virus-based replicons have been used to increase the availability of DRT, but targeted gene replacement in plants still remains very challenging^{1,3–8}.

RNA TT-HDR has been reported in yeast and human cells^{9–12}. RNA templates may be favorable for HDR because RNA:DNA hybrids are more stable than DNA:DNA duplexes¹³. However, TT-HDR has not been applied for genome engineering in plants. Because RNA transcripts can be produced in large amounts by transcription in vivo, we hypothesized that TT-HDR combined with a programmable nuclease might enable gene replacement by HDR in plants. It has been reported that a chimeric sgRNA can serve as both a guide RNA and a DRT¹⁴. However, it was not clear whether the events that the researchers detected were derived from HDR using RNA templates¹⁴. We opted to use Cpf1 nuclease rather than SpCas9 nuclease to test TT-HDR in plants because Cpf1 has dual activities. Cpf1 can process the precursor crRNA into mature crRNA as well

as using the crRNA to guide target DNA cleavage^{15,16}. Furthermore, Cpf1 cleavage produces 5'-protruding sticky ends, which may facilitate HDR¹⁶. LbCpf1 from *Lachnospiraceae* bacterium ND 2006 is an efficient Cpf1 editor in human and plant cells^{17–20}.

To test whether TT-HDR works in plants, we developed a ribonucleoprotein (RNP) system to replace the rice *ALS* gene with a mutated version (Fig. 1a). *ALS* catalyzes the first step in the biosynthesis of branched-chain amino acids and is a main target of herbicides²¹. W548L and S627I mutations in *ALS* render rice plants resistant to ALS-inhibiting herbicides⁷. These substitutions cannot be introduced by base-editing owing to a lack of useable PAM sites^{22–24}. We designed two crRNAs to enable LbCpf1 to remove a fragment from wild-type *ALS* (Fig. 1a). We also modified the crRNA target sequences so that the introduced mutant *ALS* fragments can no longer be released by the same LbCpf1–crRNAs (Fig. 1a). We designed a DRT that contains all of the intended mutations and two homologous arms (Fig. 1b). We used ribozyme-based technology²⁵ to produce two crRNAs and RNA transcripts of DRTs in vitro from a single transcript (Fig. 1c). The two ribozyme–crRNA–ribozyme (RCR) units and one ribozyme–DRT–ribozyme (RDR) unit were transcribed in tandem from the T7 promoter. Transcripts underwent self-cleavage to release the mature crRNAs and the DRT RNA transcripts (Fig. 1c). We used DNase I digestion to remove any DNA template from the in vitro transcription mixture. We delivered the RNP complexes, which contained recombinant LbCpf1 protein, two crRNAs, and the RNA templates, into rice calli by particle bombardment (Fig. 1c). As shown in Fig. 1d, we precisely replaced the wild-type *ALS* gene with the mutated version (see Supplementary Table 1 and Supplementary Fig. 1). We also observed partial HDR, in which only one end was replaced (Fig. 1d), suggesting that there might be template switching during the repair of DSBs²⁶.

To demonstrate unambiguously that an RNA template is used for gene targeting, we carried out DNase I, RNase H, and RNase A digestions of the intended DRT fragments, respectively. We carried out seven different sets of RNP experiments (Fig. 2a) in rice calli to test whether HDR occurred with various DRT templates, including RNA transcripts alone, DNA template and RNA transcripts, single-stranded DNA (ssDNA), and ssRNA, respectively. We used droplet digital PCR (ddPCR) to detect HDR events and to evaluate the RNP-mediated HDR efficiency (see Supplementary Fig. 2). Because ddPCR is effective only when the amplification length is less than 300 basepairs (bp), we had to evaluate the HDR efficiencies around target 1 and target 2 loci separately. It was clear that ssRNA could serve as a DRT for HDR (experiment IV) (Fig. 2b; see Supplementary Fig. 3 and Supplementary Table 2). The aver-

¹Institute of Crop Sciences, Chinese Academy of Agricultural Sciences, Beijing, China. ²National Key Laboratory of Crop Genetic Improvement and National Center of Plant Gene Research (Wuhan), Huazhong Agricultural University, Wuhan, China. ³Section of Cell and Developmental Biology, University of California, San Diego, La Jolla, CA, USA. *e-mail: yundezhao@ucsd.edu; xialanqin@caas.cn

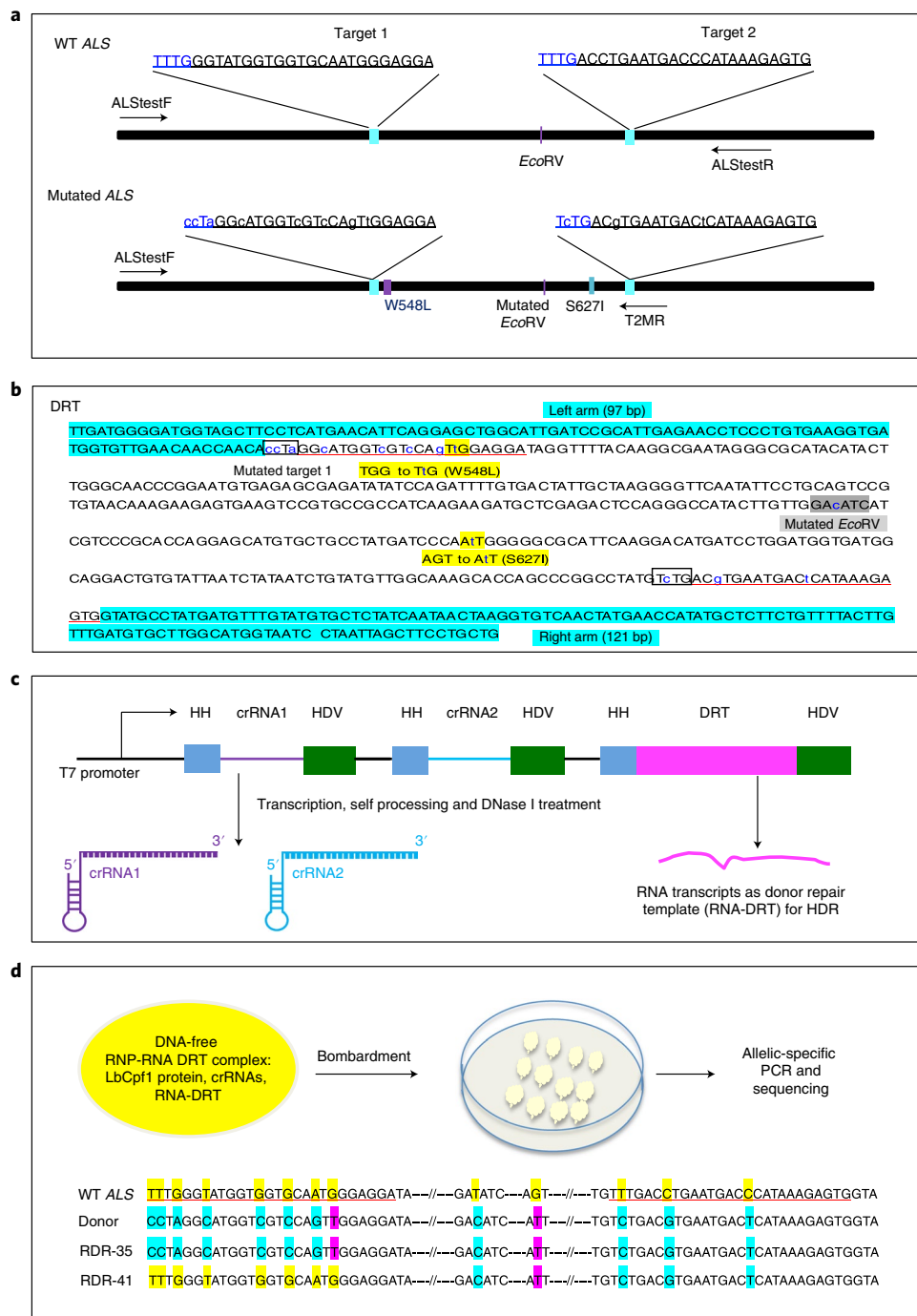


Fig. 1 | RNA TT-HDR of DSBs generated by the LbCpf1 nuclease. a, A schematic description TT-HDR-mediated precise gene replacement. The crRNA target sequences are underlined and the PAM sites are shown in blue. The wild-type ALS fragment is replaced by a mutant version harboring W548L and S627I mutations and the mutated EcoRV and PAM. ALStestF/ALStestR is the primer set designed to amplify the wild-type ALS fragment, whereas ALStestF/T2MR is designed for allelic-specific amplification of the edited ALS gene. **b**, The features and sequence of the DRT. DRT consists of the left arm (light blue), right arm (light blue), and mutated ALS fragment. Note that two point mutations of 't', which are shown in lower case in blue, are designed targeted substitutions that lead to W548L and S627I changes at the protein level, respectively. Both the two triplet codons and the encoded two mutated amino acids are shadowed in yellow. The mutated EcoRV site is shadowed in gray. Other synonymous mutations in DRT are shown in lower case in blue as well. **c**, Production of crRNAs and the RNA DRT in vitro. An array of ribozyme-flanked units is under the control of the T7 promoter. On transcription in vitro by T7 RNA polymerase, the two crRNAs and RNA transcripts of DRT are released by self-cleavage of the ribozymes. HH: hammerhead ribozyme. HDV: hepatitis delta virus ribozyme. **d**, CRISPR-Cpf1-RNP-mediated TT-HDR in rice calli. Recombinant LbCpf1 proteins and DNA-free crRNAs and RNA DRT transcripts are pre-assembled to form a DNA-free RNP-RNA DRT complex in vitro. These active RNP-RNA DRT complexes are delivered to rice calli via bombardment. PCR products are amplified by allele-specific primer set ALStestF/T2MR as described in **a**. Sequencing results of the representative TT-HDR events indicate that the callus RDR35 had undergone precise HDR, whereas the callus RDR41 had undergone partial HDR. The sequences shadowed in yellow and light blue represent the same bases as those of the wild-type and the designed DRT, respectively. Specifically, the sequences shadowed in pink indicate the desired targeted substitutions. The experiments were conducted with three biological replicates. The partial HDR (RDR41) was from the first transformation and the precise HDR (RDR35) was from the third transformation.

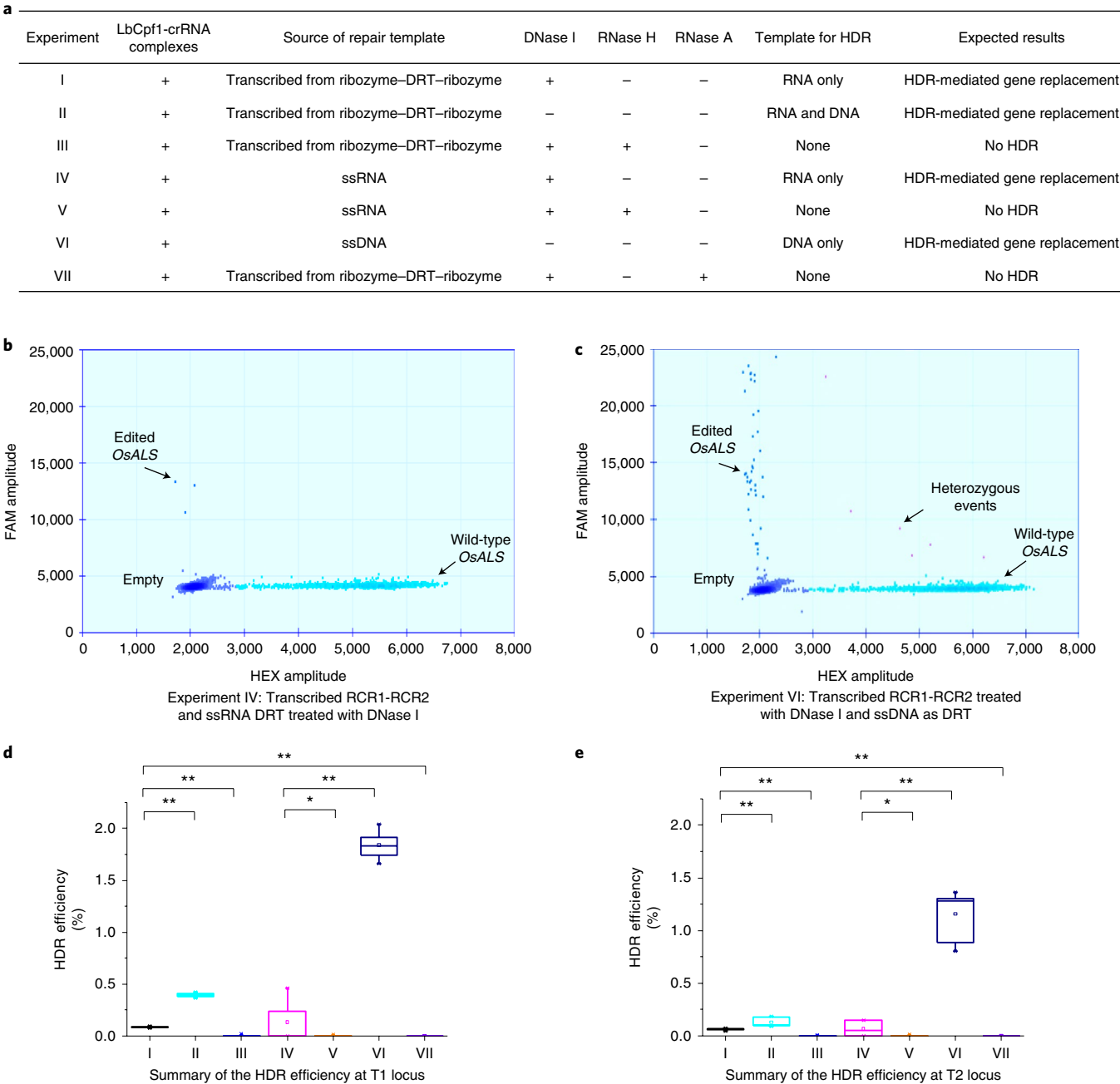
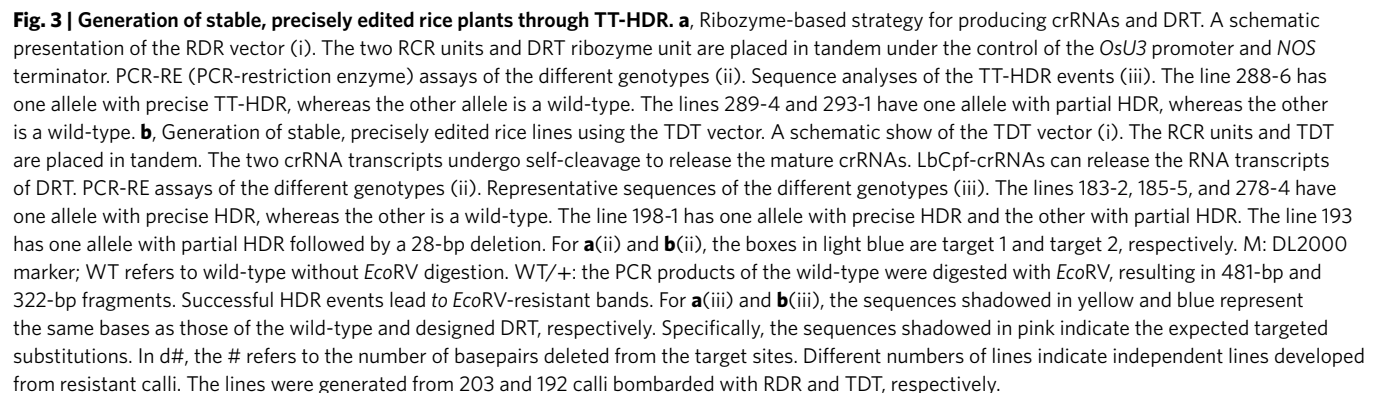


Fig. 2 | Comparison of RNP-mediated HDR efficiencies of various sources of DRTs through ddPCR. a, RNP-mediated HDR using various sources of DRTs. After transcription, the DRTs were digested by DNase I, RNase H, RNase A, or a combination of enzymes, respectively. **b,c**, Two-dimensional plots of droplets measured for fluorescence signal (amplitude indicated on y axis) emitted from edited OsALS gene (FAM labeled; positive droplets are in blue) or the wild-type OsALS gene (HEX labeled; positive droplets are in light blue) in target 1. Negative droplets are shown in black. Droplets (heterozygous events) containing both fluorescent probes are pink. The ssRNA serves as a DRT (experiment IV) (**b**). Bombardment of the RNP complex to rice calli using the transcribed RCR1-RCR2 treated with DNase I and the ssRNAs as DRTs generates HDR events. The ssDNA is an efficient HDR repair template (experiment VI) (**c**). **d,e**, Box-and-whisker plots of the HDR efficiencies of different sources of DRTs at target 1 (**d**) and target 2 (**e**). Center lines of box-and-whisker plots refer to the median of the samples. Limits of box-and-whisker plots mean maximum and minimum values of the samples. Whiskers indicate the variability outside the upper and lower quartiles. The HDR efficiencies were calculated from $n = 9$ biological replicates. Student's two-tailed t -test was performed, $**P < 0.01$ and $*P < 0.05$. The Roman numerals under the x axis correspond to the experiments described in **a**. Digestions with both RNase and DNase (experiments III, V, and VII) abolish HDR. Either DNA or RNA can serve as a repair template for HDR (experiments I, II, IV, and VI). T1: target 1. T2: target 2.

age efficiencies with ssRNA DRT (experiment IV) were around 0.13% and 0.07% at target 1 and target 2 separately (Fig. 2b and see Supplementary Table 2), whereas the average efficiencies with ssDNA DRT (experiment VI) at target 1 and target 2 were around 1.84% and 1.16%, respectively (Fig. 2c,d; see Supplementary Table 2).

As shown in Fig. 2d,e, RNA transcripts alone (experiment I, in which DNA was removed by DNase I digestion) could achieve HDR and the average efficiencies at target 1 and 2 were 0.09%, and 0.06%, respectively. Without DNase I treatment (experiment II), the average HDR efficiency was much higher (around 0.39% and



0.13% for target 1 and 2, respectively), suggesting that the availability of both DNA and RNA DRTs made HDR more effective (Fig. 2d,e; see Supplementary Table 2). We also digested DRT transcripts with either RNase A or RNase H (Fig. 2a), which degrades RNA non-specifically and removes RNA from the RNA–DNA duplexes, respectively, to determine whether HDR depends on RNA transcripts. Removal of RNA DRTs (experiments III, V, and VII) abolished HDR (Fig. 2a,d,e and see Supplementary Table 2).

Encouraged by the results of experiment II (Fig. 2a,d,e), which uses DNA and RNA transcripts as DRTs, we tested whether we could achieve HDR in rice by placing all of the HDR components in a single expression cassette (Fig. 3). Because RNA transcripts are often processed, modified, and transported into the cytosol, we used two strategies to ensure that RNA transcripts stay in the nucleus as templates for HDR. First, we placed two RCR units and an RDR unit in tandem under the control of the *OsU3* promoter and terminated by the NOS terminator (Fig. 3a–1 and see Supplementary Fig. 4a). When transcribed, both the mature crRNAs and the repair RNA template are released by self-cleavage of the ribozymes. This RDR strategy enables the production of the desired RNA transcripts even if the 5′ and 3′ ends of primary transcripts are modified²⁵. Second, we took advantage of the ability of Cpf1 to process its own pre-crRNA¹⁵. We flanked the DRT with two crRNA target sites and coupled it with the two RCR units in a single expression cassette (Fig. 3b–1 and see Supplementary Fig. 4b). The RNA transcripts of DRT can be released by LbCpf1-crRNAs (hereafter referred to as TDT, target–donor–target). One caveat of our TDT design is that LbCpf1-crRNAs can also release the DNA DRT fragment, making it difficult to distinguish between DNA and RNA DRTs. To clarify the source of DRT, we also constructed a vector named control, which produces two crRNAs from two tandem RCRs and DRT flanked with Cpf1 targets, but lacks a promoter (which means that the DRT cannot be transcribed). The DRT in the control vector can be released only by the activity of LbCpf1-crRNAs (see Supplementary Fig. 4c).

To investigate whether the three constructs (RDR, TDT, and control) can achieve TT-HDR-mediated, targeted gene replacement in rice without co-bombardment of any additional free DNA DRTs, we introduced these vectors into rice (*Japonica* cv. Zhonghua 11) calli by particle bombardment. For RDR, TDT, and the control vectors, a total of 203, 192, and 139 calli were bombarded, respectively. The calli that survived one round of hygromycin selection were transferred on to the induction media with 0.4 μmol l⁻¹ bispyribac-sodium. Then, the plants recovered from regeneration media with 0.4 μmol l⁻¹ bispyribac-sodium were used for PCR and PCR-RE digestion assay. PCR primer set ALSTestF/R was designed to amplify an *ALS* fragment from both the wild-type *ALS* locus and the edited *ALS*, but not from the plasmids (Fig. 3a(ii) and see Supplementary Table 1). All plantlets developed from one callus were treated as a pool. The plantlets in a pool that gave PCR-RE patterns different to those of the wild-type were then transferred to soil individually and further analyzed by PCR-RE and sequencing. No obvious phenotypic variations were observed between the lines and wild-type plants. In total, 58, 87, and 32 plants developed from 19, 20, and 8 bispyribac-sodium-resistant calli for the 3 treatments, respectively, were selected for further analyses (see Supplementary Table 3).

For the RDR vector (Fig. 3a(i) and see Supplementary Fig. 4a), we observed three HDR genotypes (see Supplementary Table 3). Line 288-6 was heterozygous with one allele of precise gene replacement and one wild-type (line 288-6) (Fig. 3a(ii),(iii) and see Supplementary Fig. 5). Line 289-4 had one allele with the expected substitutions around both target 1 and at the W548L locus, whereas the other allele was wild-type (Fig. 3a(ii),(iii), and see Supplementary Fig. 5). Line 291-3 had only one allele with the expected substitutions around target 2 (Fig. 3a(ii),(iii) and see Supplementary Fig. 5).

The efficiency of precise HDR was 1.7% (1/58) (see Supplementary Table 3). In this vector, DRT flanked with ribozymes could be released at the RNA level through self-cleavage. The achievement of the precise HDR event in this experiment clearly demonstrated that TT-HDR was feasible and could be employed for targeted gene replacement in plants.

For the TDT vector (Fig. 3b(i) and see Supplementary Fig. 4b), of the 87 plants recovered, we identified 4 independent heterozygous lines with 1 allele containing the expected precise gene replacement (lines 183-2, 185-5, 198-1, and 278-4), whereas the other allele was either wild-type or had partial HDR at the S627I locus (line 198-1) (Fig. 3b(ii),(iii) and see Supplementary Table 3 and Supplementary Fig. 5). We also observed that another line had the expected substitutions at both W548L and S627I loci, but with a 28-bp deletion around target 2 (line 193) (Fig. 3b(ii),(iii) and see Supplementary Fig. 5). The efficiency of precise HDR was 4.6% (4/87) (see Supplementary Table 3), indicating that our strategy efficiently achieved gene replacement. The higher frequency of HDR events in this experiment may be due to the fact that the DRT flanked with target sites could be released by LbCpf1-crRNA at both the DNA and the RNA levels.

Among the 32 plants generated from the control vector (see Supplementary Fig. 4c), none underwent any HDR events. Unlike in the TDR vector experiments (Fig. 3b(i)), DRT from the control vector could be released only by LbCpf1-crRNA acting on the DNA. These results, together with our observations in RNP assays in rice calli, further support the notion that TT-HDR occurs in plant cells.

We also evaluated whether *Agrobacterium*-mediated transformation of RDR and TDT vectors could enable TT-HDR in rice. Each vector was transformed into about 300 calli. The RDR vector (see Supplementary Fig. 4a) produced 17 plants, but no HDR events were observed (see Supplementary Table 4). The TDT vector (see Supplementary Fig. 4b) resulted in two partial HDR events among the 35 T₀ plants tested (see Supplementary Table 4). The HDR efficiency could perhaps be improved by using stronger promoters to produce larger quantities of RNA transcripts.

To analyze the stability and heritability of the HDR events, we analyzed T₁ generation edited plants. The edited loci in all of the analyzed lines, except for lines 183-2 and 198-1, which died after transferring into soil, displayed mendelian segregation (see Supplementary Table 5). Furthermore, transgene-free lines with precisely edited *ALS* loci were recovered after segregation in the T₁ generation (data not shown). Moreover, no off-target effects were detected at the potential off-target sites (CRISPR-GE, <http://skl.scau.edu.cn/>) in these tested lines (see Supplementary Table 6).

In summary, we have demonstrated that RNA transcripts can serve as repair templates for HDR in rice, thereby greatly expanding our ability to improve agriculturally important traits. Our TT-HDR technology makes DNA-free HDR feasible, and provides another boost to the potential commercialization of crops with improved traits using CRISPR-mediated HDR technology.

Received: 29 January 2018; Accepted: 11 February 2019;
Published online: 18 March 2019

References

1. Svitashv, S., Schwartz, C., Lenderts, B., Young, J. K. & Mark, A. C. Genome editing in maize directed by CRISPR–Cas9 ribonucleoprotein complexes. *Nat. Commun.* **7**, 13274 (2016).
2. Puchta, H. Repair of genomic double-strand breaks in somatic plant cells by one-sided invasion of homologous sequences. *Plant J.* **13**, 331–339 (1998).
3. Cermak, T., Baltes, N. J., Cegan, R., Zhang, Y. & Voytas, D. F. High-frequency, precise modification of the tomato genome. *Genome Biol.* **16**, 232 (2015).
4. Gil-Humanes, J. et al. High-efficiency gene targeting in hexaploid wheat using DNA replicons and CRISPR/Cas9. *Plant J.* **89**, 1251–1262 (2017).
5. Sauer, N. J. et al. Oligonucleotide-mediated genome editing provides precision and function to engineered nucleases and antibiotics in plants. *Plant Physiol.* **170**, 1917–1928 (2016).

6. Shi, J. et al. ARGOS8 variants generated by CRISPR-Cas9 improve maize grain yield under field drought stress conditions. *Plant Biotechnol. J.* **15**, 207–216 (2017).
7. Sun, Y. et al. Engineering herbicide-resistant rice plants through CRISPR/Cas9-mediated homologous recombination of acetolactate synthase. *Mol. Plant* **9**, 628–631 (2016).
8. Wang, M. et al. Gene targeting by homology-directed repair in rice using a geminivirus-based CRISPR/Cas9 system. *Mol. Plant* **10**, 1007–1010 (2017).
9. Derr, L. K., Strathern, J. N. & Garfinkel, D. J. RNA-mediated recombination in *S. cerevisiae*. *Cell* **67**, 355–364 (1991).
10. Nowacki, M. et al. RNA-mediated epigenetic programming of a genome-rearrangement pathway. *Nature* **451**, 153–158 (2007).
11. Storici, F., Bebenek, K., Kunkel, T. A., Gordenin, D. A. & Resnick, M. A. RNA-templated DNA repair. *Nature* **447**, 338–341 (2007).
12. Keskin, H. et al. Transcript-RNA-templated DNA recombination and repair. *Nature* **515**, 436–439 (2014).
13. Chien, Y. H. & Davidson, N. RNA:DNA hybrids are more stable than DNA:DNA duplexes in concentrated perchlorate and trichloroacetate solutions. *Nucleic Acids Res.* **5**, 1627–1637 (1978).
14. Butt, H. et al. Efficient CRISPR/Cas9-mediated genome editing using a chimeric single-guide RNA molecule. *Front. Plant Sci.* **8**, 1441 (2017).
15. Fonfara, I., Richter, H., Bratovič, M., Le Rhun, A. & Charpentier, E. The CRISPR-associated DNA-cleaving enzyme Cpf1 also processes precursor CRISPR RNA. *Nature* **532**, 517–521 (2016).
16. Zetsche, B. et al. Cpf1 is a single RNA-guided endonuclease of a class 2 CRISPR-cas system. *Cell* **163**, 759–771 (2015).
17. Kim, D. et al. Genome-wide analysis reveals specificities of Cpf1 endonucleases in human cells. *Nat. Biotechnol.* **34**, 863–868 (2016).
18. Kim, H. et al. CRISPR/Cpf1-mediated DNA-free plant genome editing. *Nat. Commun.* **8**, 14406 (2017).
19. Tang, X. et al. A CRISPR–Cpf1 system for efficient genome editing and transcriptional repression in plants. *Nat. Plants* **3**, 17018 (2017).
20. Zetsche, B. et al. Multiplex gene editing by CRISPR-Cpf1 using a single crRNA array. *Nat. Biotechnol.* **35**, 31–34 (2017).
21. Mazur, B. J., Chui, C. F. & Smith, J. K. Isolation and characterization of plant genes coding for acetolactate synthase, the target enzyme for two classes of herbicides. *Plant Physiol.* **85**, 1110–1117 (1987).
22. Komor, A. C., Kim, Y. B., Packer, M. S., Zuris, J. A. & Liu, D. R. Programmable editing of a target base in genomic DNA without double-stranded DNA cleavage. *Nature* **533**, 420–424 (2016).
23. Li, J., Sun, Y., Du, J., Zhao, Y. & Xia, L. Generation of targeted point mutations in rice by a modified CRISPR/Cas9 system. *Mol. Plant* **10**, 526–529 (2017).
24. Shimatani, Z. et al. Targeted base editing in rice and tomato using a CRISPR-Cas9 cytidine deaminase fusion. *Nat. Biotechnol.* **35**, 441–443 (2017).
25. Gao, Y. & Zhao, Y. Self-processing of ribozyme-flanked RNAs into guide RNAs in vitro and in vivo for CRISPR-mediated genome editing. *J. Integr. Plant Biol.* **56**, 343–349 (2014).
26. Paix, A. et al. Precision genome editing using synthesis-dependent repair of Cas9-induced DNA breaks. *Proc. Natl Acad. Sci. USA* **114**, E10745–E10754 (2017).

Acknowledgments

We thank J.-K. Zhu for the LbCpf1 plasmid. We thank C.-Y. Wu, whose lab provided the rice transformation service. This work is partly funded by the Ministry of Agriculture and Rural Affairs of China (grant no. 2018ZX0801003B to L.X. and Y.H.), the Ministry of Science and Technology of China (grant no. 2016YFD0100500 to LX), the Ministry of Agriculture of China (grant no. 2016ZX08010003 to L.X.), and the Central Non-Profit Fundamental Research Funding supported by the Institute of Crop Sciences, Chinese Academy of Agricultural Sciences (S2018QY05 to L.X.).

Author contributions

L.X. and Y.Z. conceived the project. S.L., J.L., Y.H., M.X., J.Z., and W.D. performed the experiments. L.X. and Y.Z. wrote the manuscript.

Competing interests

The authors have filed a patent application based on the system developed in this paper.

Additional information

Supplementary information is available for this paper at <https://doi.org/10.1038/s41587-019-0065-7>.

Reprints and permissions information is available at www.nature.com/reprints.

Correspondence and requests for materials should be addressed to Y.Z. or L.X.

Publisher's note: Springer Nature remains neutral with regard to jurisdictional claims in published maps and institutional affiliations.

© The Author(s), under exclusive licence to Springer Nature America, Inc. 2019

Methods

Synthesis of the designed DTR. We designed a DRT fragment that contained the following features (see Fig. 1b). First, the fragment contained the desired mutations (W548L and S627I substitutions) in the *ALS* gene, which render rice plants resistant to ALS-inhibiting herbicides. Second, the donor fragment had several synonymous substitutions at the target 1 and target 2 loci, respectively, which prevent the introduced replacement from further cleavage by LbCpf1-crRNAs once HDR has been successfully achieved. Third, the 381-bp core sequences in the DRT were flanked with a 97-bp left homologous arm and a 121-bp right homologous arm, respectively, which are identical to the stretches of wild-type *ALS* sequences. Moreover, an *EcoRV* restriction site between the two target sites in the donor fragment was abolished to facilitate detection of gene replacement events. Finally, the designed DRT fragment was synthesized by BGI (Beijing Genomics Institute).

Preparation of ssDNA and ssRNA DTR. The ssDNA fragment was amplified using primer set donorF/donorR (see Supplementary Table 1) from the synthesized DRT by asymmetric PCR, and the products were purified using Columns (Tiangen) followed by ethanol precipitation. A T7-DRT DNA fragment was amplified using primer set T7-donorF/T7-donorR from a synthesized DRT, and was used as the template for in vitro transcription of ssRNA (see Supplementary Table 1). The in vitro transcription was performed using the HiScribe T7 Quick High Yield RNA Synthesis Kit (New England Biolabs). The in vitro transcribed ssRNAs were subjected to DNase I, RNase H, or RNase A treatments as described in the manufacturer's protocol, and further purified using NucAway Spin Columns (Life Technologies Inc.).

Preparation of RCR–RCR2–RDR transcripts. The RCR units were assembled through overlapping PCR reactions. To generate RCR1, we conducted the first round of PCR (PCR1) using RCR1F2/RCR-common-R primer set and the plasmid pRS316-RGR-GFP^{25,27} as a template. The second PCR reaction used the primer set RCRF1/RCR-common-R and the product from PCR1 as the template (see Supplementary Table 1). The same procedure was used to obtain the RCR2 unit with the primer set RCR2-F2/RCR-common-R and RCRF1/RCR-common-R, respectively (see Supplementary Table 1). The RCR1–RCR2 unit was obtained through three rounds of overlapping PCR reactions. The first PCR was performed with primer set RCR-Common-F/RCR1-10 random-R using RCR1 unit as the template (see Supplementary Table 1). The second PCR was performed with primer set RCR2-10 random-F/SacI-RCR2-R using the RCR2 unit as the template (see Supplementary Table 1). Products of PCR1 and -2 were used as templates for the third PCR reaction with the primer set RCR-Common-F/SacI-RCR2-R to generate the RCR1–RCR2 unit. The RCR1–RCR2 unit was cloned into a pEASY-Blunt vector (TransGen Biotech) for sequencing.

The RDR-Nos fragment was obtained through five rounds of overlapping PCR reactions. The hammerhead ribozyme (HH) fragment was obtained by PCR through annealed primer set HHF/HHR (see Supplementary Table 1). The second PCR was performed with primer set donor-HH-F/donor-HH-R using the synthesized DRT as template (see Supplementary Table 1). The third PCR was performed using primer set HDVF/HDVR with the plasmid pRS316-RGR-GFP^{25,27} as the template (see Supplementary Table 1). The fourth PCR was performed using primer set Nos-HDVF/Not-NosR with the plasmid pCXUN-Cas9⁷ as template (see Supplementary Table 1). Products of PCR1–4 were used as templates for the fifth PCR reaction, with the primer set Not-HHF/Not-NosR to generate the RDR-Nos fragment (see Supplementary Table 1). The fragment was cloned into the *NotI* site of the pEASY-RCR1-RCR vector using the Assembly Kit (TransGen Biotech). The final plasmid was named pEASY-RCR1-RCR-RDR-Nos. PCR primers for vector construction are listed in Supplementary Table 1.

PCR products named RCR1–RCR2–RDR were amplified from the vector pEASY-RCR1-RCR-RDR-Nos using the appropriate primer set, and used as the templates for in vitro transcription (see Supplementary Table 1). In vitro transcription was performed using the HiScribe T7 Quick High Yield RNA Synthesis Kit (New England Biolabs). The in vitro transcribed products were subjected to DNase I, RNase H, or RNase A treatments as described in the manufacturer's protocol and further purified using NucAway Spin Columns (Life Technologies Inc.).

An RNP complex comprising LbCpf1-crRNA and RNA transcripts was generated as follows: 10 µg LbCpf1 protein and 10 µg RNA transcripts, including crRNAs and DRT RNA transcripts, in a 1:1 molar ratio were pre-mixed in 1×NEBuffer 3 supplemented with 1 µl RNase inhibitor (New England Biolabs) to the final volume of 20 µl, and incubated at room temperature for 15 min.

CRISPR/Cpf1-RNP-mediated TT-HDR using RNA transcripts as the DTR in rice calli. The pre-assembled RNPs were precipitated on to 0.6-mm gold particles (Bio-Rad) using a water-soluble cationic lipid TransIT-2020 (Mirus) as follows: 50 µl of gold particles (water suspension of 20 mg ml⁻¹) and 2 µl TransIT-2020 water solution were added to 20 µl pre-assembled RNPs, mixed gently, and incubated on ice for 10 min. RNP/RNA-coated gold particles were then pelleted in a microfuge at 8,000g for 30 s and the supernatant discarded. The pellet was re-suspended in 50 µl sterile water by brief sonication. Immediately after sonication, coated gold particles were loaded on to a macro-carrier (10 µl each) and allowed to air dry. Calli of a *Japonica* rice (cv. Zhonghua 11) developed from mature embryos were bombarded

using a PDS1000/He Gun (Bio-Rad) with a rupture pressure of 900 psi following the protocol described previously²⁸.

For each treatment, we bombarded ten calli with three biological replicates. Thirty-six hours after bombardment, DNA from the calli was extracted using a DNA Quick Plant System (Tiangen). PCR amplification was performed using EASY Taq polymerase (TransGen Biotech) by using 200 ng of genomic DNA as a template. Each callus was tested individually by PCR and sequencing. The PCR products were generated using the allele-specific primer set ALSTestF/T2MR (see Supplementary Table 1) with up-stream primer located in the genome sequence of the *ALS* gene outside the left homologous arm, whereas the down-stream primer was an allele-specific primer (see Fig. 1a and Supplementary Fig. 1). The obtained amplicons were cloned into the cloning vector pEASY-Blunt (TransGen Biotech). At least ten positive colonies for each sample were sequenced.

Droplet digital PCR. Primers and probes were designed following the criteria specified by the instrument manufacturer. Candidate primers were designed using Primer 5 with manually adjusted settings to an annealing temperature of 56 °C, while fluorescently labeled probes for amplicon detection were selected to have annealing temperatures of ≥ 59 °C. The edited *OsALS* gene probes were labeled with 5'-FAM (6-fluorescein; Beijing Genomics Institute) and the wild-type *OsALS* gene probes were labeled with 5'-HEX (hexachlorofluorescein; Beijing Genomics Institute) (see Supplementary Table 1 and Fig. 2). Both types of probes were quenched with Iowa Black Hole Quencher 1 (The Beijing Genomics Institute).

For each sample tested, a ddPCR cocktail was generated that contained 11 µl 2x ddPCR Supermix for Probes (no dUTP) (Bio-Rad Laboratories), 900 nmol l⁻¹ of each primer pair and 250 nmol l⁻¹ of each probe. Genome DNA 25 ng was added to the mixture and the final volume was adjusted to 22 µl with sterile ultrapure water. Droplets were produced from 20 µl of the complete reaction mixture, drawn together with 70 µl Bio-Rad Droplet Generation Oil in the microcapillary droplet generator cartridge, following the manufacturer's instructions. Droplets (40 µl) were transferred slowly and carefully from the droplet generation cassette to ddPCR 96-well plates, sealed with pierceable foil and placed into the thermocycler. The amplification program incorporated an initial 95 °C denaturation for 10 min, followed by 40 cycles of 94 °C (30 s) and 56 °C for 1 min. The 40 cycles were followed by a step at 98 °C for 10 min and then at 4 °C. A temperature ramp rate of 2 °C s⁻¹ was utilized between all changes in temperature to follow the instrument manufacturer's guidelines. After amplification, the samples were transferred to a Bio-Rad QX200 droplet reader.

Detection of successful HDR events and evaluation of the HDR efficiencies by ddPCR at target 1 and target 2 loci, respectively. For every treatment, 1 µg genomic DNA from each callus (total ten calli for each treatment) was pooled to evaluate the frequency of the HDR events. As a result of the limit of amplification length using ddPCR, mutated target 1 and mutated target 2 were detected separately. At the target 1 locus, the T1F/T1R primer set was used to amplify the products, and the probes T1-Edit and T1-WT were used to detect PCR products of the edited and wild-type *OsALS* gene, respectively (see Supplementary Table 1 and Supplementary Fig. 2). We designed T1F, which is located on the genome outside the left homologous arm of DRT, whereas T1R is inside the DRT (see Supplementary Fig. 2). At the target 2 locus, the same experiment was performed with primer pair T2F/T2R and probes T2-Edit and T2-WT (see Supplementary Table 1 and Supplementary Fig. 2). Also, we designed T2F which is located inside the DRT, whereas T2R is located on the genome outside the right homologous arm of DRT (see Supplementary Fig. 2). Droplets were counted and the frequencies of HDR events generated by using the Bio-Rad QuantaSoft software (v1.6.6.0320) (see Supplementary Fig. 3).

For each sample, the frequency of HDR events was calculated. A box-and-whisker plot was made based on the ratio of HDR events using the software OriginPro 9 (OriginLab). To compare the efficiency of different treatments, a Student's *t*-test was employed to evaluate the significance of the difference between two experiments using OriginPro 9. Significance (*P* value) was evaluated at the 1% level for all comparisons. For each experiment, the standard deviation of the mean was calculated, based on nine biological replicates (see Supplementary Table 2).

Construction of the CRISPR/LbCpf1-related vectors. The pCXUN-LbCpf1 vector used in this study was constructed based on the vector pCXUN-Cas9⁷ by replacing the ubiquitin-Cas9 with the ubiquitin-LbCpf1 from the LbCpf1-OsUbe²⁹. The backbone of pCXUN-Ubi-LbCpf1-Nos contains a hygromycin-resistant gene (*hpt*). The *SacI* and *KpnI* sites in pCXUN-Ubi-LbCpf1-Nos were used for introducing the OsU3-RCR1-RCR2 expression cassette and the DNA DRT, respectively (see Supplementary Fig. 4).

OsU3 promoter was amplified using primer set OsU3F/OsU3R (see Supplementary Table 1) from the plasmid pCXUN-Cas9-OsU3⁷. As the *OsU3* promoter was used in this experiment, we also placed an adenine nucleotide before the first nucleotide of the RCR sequences. The full-length OsU3-RCR1-RCR2 cassette was obtained through two rounds of overlapping PCR reactions. The first PCR was performed with primer set OsU3F/OsU3-RCR1R, using the *OsU3* promoter sequence as the template (see Supplementary Table 1). The second PCR was performed with the primer set RCR-Common-F/SacI-RCR2-R, using the vector pEASY-RCR1-RCR as the template (see Supplementary Table 1). Products

of PCR1 and -2 were used as templates for the third PCR reaction, with the primer set SacI-OsU3-F/SacI-RCR2-R, to generate the OsU3-RCR1-RCR2 cassette. At the 5'-end of the primer pair of SacI-OsU3-F/SacI-RCR2-R, the sequences are homologous to the sequences outside the SacI site in pCXUN-Ubi-LbCpf1-Nos. The OsU3-RCR1-RCR2 fragment was subsequently cloned into the SacI-linearized pCXUN-Ubi-LbCpf1-Nos, by using the pEASY-Uni Seamless Cloning and Assembly Kit (TransGen Biotech). The vector harboring both Ubi-LbCpf1-Nos and OsU3-RCR1-RCR2 was named pCXUN-OsU3-RCR1-RCR2-Ubi-LbCpf1-Nos.

The vector pCXUN-OsU3-RCR1-RCR2-RDR-Nos-Ubi-LbCpf1-Nos was obtained by overlapping PCR reactions. The Kpn-RDR-Nos fragment was amplified with the primer set Kpn-HHF/Kpn-NosR from the vector pEASY-RCR1-RCR2-RDR-Nos as the template (see Supplementary Table 1). The fragment was cloned into the KpnI site of pCXUN-OsU3-RCR1-RCR2-Ubi-LbCpf1-Nos using the Assembly Kit (TransGen Biotech). The final plasmid was named pCXUN-OsU3-RCR1-RCR2-RDR-Nos-Ubi-LbCpf1-Nos (see Supplementary Fig. 4a). PCR primers for vector construction are listed in Supplementary Table 1.

The vector pCXUN-OsU3-RCR1-RCR2-armed donor (with targets)-Nos-Ubi-LbCpf1-Nos was obtained by overlapping PCR reactions. The fragment of donor (with targets)-Nos was assembled through overlapping PCR reactions. PCR1 products were obtained by PCR using the primer set Kpn-donorF/donorR with a synthesized donor fragment as the template, and PCR2 was performed with the primer set Nos-donorF/Kpn-NosR using the plasmid pCXUN-Ubi-LbCpf1-Nos as the template (see Supplementary Table 1). Products of PCR1 and -2 were used as templates for the third rounds of PCR with the primer set Kpn-donorF/Kpn-NosR, to generate the donor-Nos fragment. The fragment was cloned into the KpnI site of pCXUN-OsU3-RCR1-RCR2-Ubi-LbCpf1-Nos using the Assembly Kit (TransGen Biotech). The final plasmid was named pCXUN-OsU3-RCR1-RCR2-armed donor (with targets)-Nos-Ubi-LbCpf1-Nos (see Supplementary Fig. 4b). PCR primers for vector construction are listed in Supplementary Table 1.

To generate a control plasmid, a donor fragment was amplified by PCR using the primer set Pme-donorF/Pme-donorR with the synthesized donor fragment as the template, and cloned into the PmeI site of pCXUN-OsU3-RCR1-RCR2, which is located at the other side of the Ubi-LbCpf1-Nos cassette, by using the Assembly Kit (TransGen Biotech). The final plasmid was named pCXUN-OsU3-RCR1-RCR2-Ubi-LbCpf1-Nos-armed donor (with targets) (see Supplementary Fig. 4c). PCR primers for vector construction are listed in Supplementary Table 1.

Rice transformation. For induction of rice calli from mature seeds, the mature seeds were first sterilized using 75% alcohol and 20% NaClO, followed by washes with sterilized deionized water. Then, the sterilized rice seeds were placed on to the induction medium for about 1 month at 28°C in the dark. Finally, after subculture, the induced rice calli were used for transformation.

For rice transformation by bombardment, the vectors pCXUN-OsU3-RCR1-RCR2-RDR-Nos-Ubi-LbCpf1-Nos, pCXUN-OsU3-RCR1-RCR2-armed donor (with targets)-Nos-Ubi-LbCpf1-Nos, and pCXUN-OsU3-RCR1-RCR2-Ubi-LbCpf1-Nos-armed donor (with targets) (see Supplementary Fig. 4) were linearized by SacII, then transformed into calli of a *Japonica* rice (cv. Zhonghua 11) by particle bombardment, followed by the protocol described previously²⁸. Particle bombardments were performed using a PDS1000/He particle bombardment system (Bio-Rad).

For rice *Agrobacterium* transformation, the vectors RDR (pCXUN-OsU3-RCR1-RCR2-RDR-Nos-Ubi-LbCpf1-Nos) (see Supplementary Fig. 4a) and TDT (pCXUN-OsU3-RCR1-RCR2-armed donor (with targets)-Nos-Ubi-LbCpf1-Nos) (see Supplementary Fig. 4b) were transformed into calli of a *Japonica* rice (cv. Zhonghua 11) by *Agrobacterium*-mediated transformation as described previously³⁰.

After transformation, the calli were selected on first selection medium containing 50 mg l⁻¹ hygromycin for 2 weeks at 28°C in the dark, to allow the growth of calli with the construct, either transiently expressed or stably integrated. Then the well-grown calli were transferred to the second selection medium containing 0.4 μmol l⁻¹ bispyribac-sodium at 28°C in the dark for 2 weeks. After two rounds of selection, the vigorously resistant calli were transferred to

regeneration media with 0.4 μmol l⁻¹ bispyribac-sodium for about 3–4 weeks to regenerate green seedlings at 28°C in the light (16 h light:8 h dark). After regeneration, the green seedlings were transferred to the rooting medium to generate green plants at 28°C in the light (16 h light:8 h dark).

Molecular characterization of the edited plants. Rice genomic DNA from leaf tissues was extracted using a DNA Quick Plant System (Tiangen). PCR amplification was performed using EASY Taq polymerase (TransGen Biotech) and 200 ng of genomic DNA as a template. All plants were tested individually with PCR-RE and sequencing. The PCR products amplified by the primer pair ALSTestF/ALSTestR (see Supplementary Table 1) were digested with *EcoRV* and then directly sequenced to screen for the plants with a modified *ALS* gene. The sequence chromatograms were analyzed using a web-based tool (<http://dsdecode.scgene.com/>) to confirm the genotype and zygosity of the tested plants³¹. Some PCR products were also cloned into the cloning vector pEASY-Blunt Zero (TransGen Biotech), and at least ten positive colonies for each sample were sequenced. Primers for detection of the presence of *LbCpf1*, *RCR*, and *hptII* are listed in Supplementary Table 1.

To investigate off-target effects, we selected three and two potential off-target sites, based on the predictions of the CRISPR-GE (<http://skl.scau.edu.cn/>), for target 1 and target 2, respectively (see Supplementary Table 5). Site-specific genomic PCR and DNA Sanger sequencing were used to determine the off-target effects. The primer sets are as listed in Supplementary Table 1.

All Sanger sequencing results are included in the Supplementary Data 1.

Segregation and statistical analysis. T₀ plants with ~30 seeds or more were harvested for segregation analysis. Genomic DNAs were extracted from T₁ seedlings using a DNA Quick Plant System (Tiangen) from leaf tissues. PCR amplification was performed using EASY Taq polymerase (TransGen Biotech) and 200 ng of genomic DNA as template. The PCR products amplified by the primer pair ALSTestF/ALSTestR (see Fig. 1a and Supplementary Table 1) were directly sequenced to perform segregation analysis of HDR events in T₁ seedlings. The PCR products amplified by the primer pair LbCpf1F/LbCpf1R (see Supplementary Table 1) were used to detect *LbCpf1* in T₁ seedlings. The χ^2 test was performed to test whether the segregations of edited events were somatic and in accordance with mendelian genetics.

Reporting Summary. Further information on research design is available in the Nature Research Reporting Summary linked to this article.

Data availability

All data supporting the findings of this study are available in the article and its Supplementary Figures and Tables. Raw Sanger sequencing data are included in Supplementary Data 1.

References

- Zhang, T., Gao, Y., Wang, R. & Zhao, Y. Production of guide RNAs in vitro and in vivo for CRISPR using ribozymes and RNA polymerase II promoters. *Bio Protoc.* **7**, e2148 (2017).
- Li, L., Qu, R., de Kochko, A., Fauquet, C. & Beachy, R. N. An improved rice transformation system using the biolistic method. *Plant Cell Rep.* **12**, 250–255 (1993).
- Wang, M., Mao, Y., Lu, Y., Tao, X. & Zhu, J.-k. Multiplex gene editing in rice using the CRISPR-Cpf1 system. *Mol. Plant* **10**, 1011–1013 (2017).
- Hiei, Y., Ohta, S., Komari, T. & Kumashiro, T. Efficient transformation of rice (*Oryza sativa* L.) mediated by *Agrobacterium* and sequence analysis of the boundaries of the T-DNA. *Plant J.* **6**, 271–282 (1994).
- Liu, W. et al. DSDcode: a web-based tool for decoding of sequencing chromatograms for genotyping of targeted mutations. *Mol. Plant* **8**, 1431–1433 (2015).

Reporting Summary

Nature Research wishes to improve the reproducibility of the work that we publish. This form provides structure for consistency and transparency in reporting. For further information on Nature Research policies, see [Authors & Referees](#) and the [Editorial Policy Checklist](#).

Statistical parameters

When statistical analyses are reported, confirm that the following items are present in the relevant location (e.g. figure legend, table legend, main text, or Methods section).

n/a Confirmed

- ☐ ☒ The exact sample size (n) for each experimental group/condition, given as a discrete number and unit of measurement
- ☐ ☒ An indication of whether measurements were taken from distinct samples or whether the same sample was measured repeatedly
- ☐ ☒ The statistical test(s) used AND whether they are one- or two-sided
Only common tests should be described solely by name; describe more complex techniques in the Methods section.
- ☐ ☒ A description of all covariates tested
- ☐ ☒ A description of any assumptions or corrections, such as tests of normality and adjustment for multiple comparisons
- ☐ ☒ A full description of the statistics including central tendency (e.g. means) or other basic estimates (e.g. regression coefficient) AND variation (e.g. standard deviation) or associated estimates of uncertainty (e.g. confidence intervals)
- ☐ ☒ For null hypothesis testing, the test statistic (e.g. F , t , r) with confidence intervals, effect sizes, degrees of freedom and P value noted
Give P values as exact values whenever suitable.
- ☒ ☐ For Bayesian analysis, information on the choice of priors and Markov chain Monte Carlo settings
- ☒ ☐ For hierarchical and complex designs, identification of the appropriate level for tests and full reporting of outcomes
- ☒ ☐ Estimates of effect sizes (e.g. Cohen's d , Pearson's r), indicating how they were calculated
- ☐ ☒ Clearly defined error bars
State explicitly what error bars represent (e.g. SD, SE, CI)

Our web collection on [statistics for biologists](#) may be useful.

Software and code

Policy information about [availability of computer code](#)

Data collection Bio-Rad QuantaSoft™ software (v1.6.6.0320)

Data analysis OriginPro 9 (OriginLab, USA).

For manuscripts utilizing custom algorithms or software that are central to the research but not yet described in published literature, software must be made available to editors/reviewers upon request. We strongly encourage code deposition in a community repository (e.g. GitHub). See the Nature Research [guidelines for submitting code & software](#) for further information.

Data

Policy information about [availability of data](#)

All manuscripts must include a [data availability statement](#). This statement should provide the following information, where applicable:

- Accession codes, unique identifiers, or web links for publicly available datasets
- A list of figures that have associated raw data
- A description of any restrictions on data availability

All data generated or analysed during this study are included in this published article (and its supplementary information files).

Field-specific reporting

Please select the best fit for your research. If you are not sure, read the appropriate sections before making your selection.

☒ Life sciences ☐ Behavioural & social sciences ☐ Ecological, evolutionary & environmental sciences

For a reference copy of the document with all sections, see [nature.com/authors/policies/ReportingSummary-flat.pdf](https://www.nature.com/authors/policies/ReportingSummary-flat.pdf)

Life sciences study design

All studies must disclose on these points even when the disclosure is negative.

Sample size	No need to pre-determine the sample size in this case. In this study, we investigate whether RNA transcripts can be used as a template. The work is more qualitative and does not rely on statistic significance.
Data exclusions	No data is excluded
Replication	Multiple transformation experiments were conducted. The results were confirmed independently by different students. Results are confirmed by DNA sequencing. Sanger sequencing files are included in supplemental files
Randomization	The transgenic events investigated were selected randomly. The transgenic plants were grouped based on different plasmids.
Blinding	Investigators were not blinded during analysis. The experiments require multiple steps, making double blind difficult. The final results are DNA sequencing, which were read by multiple people.

Reporting for specific materials, systems and methods

Materials & experimental systems

n/a	Involved in the study
<input type="checkbox"/>	<input checked="" type="checkbox"/> Unique biological materials
<input checked="" type="checkbox"/>	<input type="checkbox"/> Antibodies
<input checked="" type="checkbox"/>	<input type="checkbox"/> Eukaryotic cell lines
<input checked="" type="checkbox"/>	<input type="checkbox"/> Palaeontology
<input checked="" type="checkbox"/>	<input type="checkbox"/> Animals and other organisms
<input checked="" type="checkbox"/>	<input type="checkbox"/> Human research participants

Methods

n/a	Involved in the study
<input checked="" type="checkbox"/>	<input type="checkbox"/> ChIP-seq
<input checked="" type="checkbox"/>	<input type="checkbox"/> Flow cytometry
<input checked="" type="checkbox"/>	<input type="checkbox"/> MRI-based neuroimaging

Unique biological materials

Policy information about [availability of materials](#)

Obtaining unique materials All biological materials are available to academic researchers free of charge.